AMERICAN ACADEMY OF OPHTHALMOLOGY®

Optimizing Retinal Thermofusion in Retinal Detachment Repair

Achieving Instant Adhesion without Air Tamponade

Wilson J. Heriot, MB, BS,[1,2,3] *Andrew B. Metha, PhD, BScOptom,*[3] *Zheng He, PhD, MSci,*[3] *Jeremiah K.H. Lim, PhD,*[3,4] *Anh Hoang, BSci,*[2,3] *Tomoharu Nishimura, PhD, MD,*[3,5] *Mali Okada, MBBS,*[2] *Bang V. Bui, PhD, BSciOptom*[3]

Purpose: Rhegmatogenous retinal detachment repair by intraoperative sealing of the tear without a tamponade agent should enable faster restoration of vision and resumption of normal activities. It avoids the need for further surgery in the case of silicone oil endotamponade. This study evaluated the retinal thermofusion (RTF) retinopexy method of subretinal space dehydration before photocoagulation to create an instantaneous intraoperative retina reattachment in a preclinical model.

Design: Preclinical study.

Participants: Twenty Dutch Belt, pigmented rabbits that underwent RTF repair after experimental retinal detachment.

Methods: This ex vivo model quantified adhesion force between the retina and underlying retinal pigment epithelium and choroid after treatment of 1 retinal edge using postmortem porcine or human retina (6 × 12 mm). We compared (1) control, (2) laser photocoagulation alone, (3) dehydration alone, and (4) dehydration followed by photocoagulation (RTF). Optimized parameters for RTF were then applied in the in vivo rabbit model of retinal detachment. Animals were followed up for 14 days.

Main Outcome Measures: For this ex vivo model, we measured adhesion force and related this to tissue temperature. For the in vivo study, we assessed retinal attachment using funduscopy and histologic analysis.

Results: The ex vivo model showed that RTF repair produced significantly higher adhesion force than photocoagulation alone independent of dehydration method: warm (60° C) high airflow (50−70 ml/minute) or using laser wavelengths targeting water absorption peaks (1470 or 1940 nm) with coaxial low airflow (10−20 ml/minute). The latter approach produced a smaller footprint of dehydration. Application of RTF (1940-nm laser with coaxial airflow) in an in vivo retinal detachment model in rabbit eyes resulted in immediate retinal adhesion, achieving forces similar to those in the ex vivo experiments. Retinal thermofusion repair resulted in stable reattachment of the retina over the 2-week follow-up period.

Conclusions: We showed that a short preliminary dehydrating laser treatment of a retinal tear margin before traditional laser photocoagulation creates an immediate intraoperative waterproof retinopexy adhesion independent of tamponade and a wound-healing response. This approach potentially will allow rapid postoperative recovery regardless of the tear location and improved vision. *Ophthalmology Science 2022;2:100179* © *2022 by the American Academy of Ophthalmology. This is an open access article under the CC BY-NC-ND license (http://creativecommons.org/licenses/by-nc-nd/4.0/).*

Supplemental material available at www.ophthalmologyscience.org

The essential outcome for successful rhegmatogenous retinal detachment repair is closing the communication between the vitreous cavity and the subretinal space (SRS). Current retinopexy techniques do not create an instantaneous seal or strong retinal adhesion to the underlying retinal pigment epithelium (RPE) and choroid during surgery, as demonstrated clinically by retinal slippage during fluid−gas exchange for giant retinal tear (GRT) repair.[1] The current method for retinal detachment repair is based on century-old principles established by Jules Gonin, whereby a thermal tissue injury (heat or cold) triggers an inflammatory wound-healing reaction that binds the margin of the retinal tears to the underlying RPE and choroid.[2–5] Wound healing requires both time and continuous contact between the injured tissues to form a strong bond,[6,7] just as repair of a skin incision relies initially on sutures, tape, or other support. Currently, retinal and choroidal contact is achieved with an extraocular scleral buckle or, more commonly, vitreoretinal surgery (vitrectomy) with a gas or liquid tamponade agent.[8,9] When the tamponade is a gas,

https://doi.org/10.1016/j.xops.2022.100179
ISSN 2666-9145/22

vision can be blocked for several weeks, most patients are unable to continue working, mobility is restricted, and driving is prohibited.[10] Critically, air travel or aeromedical evacuation is prohibited because of the risk of blinding intraocular gas expansion as ambient cabin pressure decreases during ascent and flight.[11–14] Liquid tamponade agents (silicone oil or a heavier-than-water mixture with perfluorocarbon liquid) require a second procedure for removal and can be associated with a variety of complications,[15] including oil maculopathy and glaucoma. Furthermore, to achieve optimal buoyancy effect of the tamponade, patients often need to assume a certain position for up to 1 week after the procedure, particularly for inferior pathologic features. This relies on patient compliance and can be difficult in those with mobility or cognitive issues. Finally, the presence of a gas tamponade at the completion of surgery can contribute to greater risk of retinal displacement and aniseikonia.[16]

That retinal reattachment after vitrectomy without tamponade is possible was reported by Martinez-Castillo et al,[17] but others have been unable to reproduce these results reliably. Retinal detachment repair without tamponade requires a new reproducible surgical method to seal retinal tears during surgery that is preferably intuitive for trained surgeons and compatible with current vitreoretinal surgical systems.

These requirements prompted a reexamination of the basic pathophysiologic features of retinal adhesion formation (retinopexy) and led to the development of the retinal thermofusion (RTF)[18] method. This method is based on the basic principles that neither aspiration of nor displacement by agents heavier than water (such as perfluorocarbon liquid) can evacuate all the subretinal fluid (SRF) because of the physical properties of water, namely, the cohesion between water molecules and the adhesion of water molecules to a surface. Subretinal fluid is near-Newtonian with relatively weak intermolecular bonds (cohesion) holding water molecules together,[19] and these are much weaker than the adhesive force between water and surfaces. In addition, the cell membranes of the RPE and the retina are lipid and thus hydrophobic and are immiscible with water. It is proposed that the persistence of a fine layer of SRF facilitates retinal translocation and slippage during GRT repair, despite the clinical appearance that the retina has been reattached. Crucially, the fine layer of SRF maintains separation of the outer retina from the RPE such that photocoagulation coagulates both tissues sequentially and independently; the RPE and choroid are coagulated by heat generated by melanin absorption of laser energy, and the retina is coagulated indirectly by the choroidal heat transferred via the SRF. The laser coagulation of the RPE and choroid separately to the retina prevents instantaneous integration of the two such that a wound-healing process is required to create a permanent connection between the tissues.

Based on the preliminary method of RTF in which subretinal dehydration was achieved with a room temperature air stream,[18] we investigated a variety of methods to achieve SRS dehydration and measured the adhesion strength created by laser photocoagulation, both with and without SRS dehydration. We also developed a novel laser-based device comprising wavelengths that liberate water molecules from the water phase without significant elevation of tissue temperature to coagulation levels that, when combined with a low-flow coaxial airstream, achieve rapid and focal dehydration of the retinal tear margin by a process we call *photodehydration*. Photocoagulation with the same wavelength at a higher-power intensity then was performed in the dehydrated area to create the instantaneous fusion of retina with the RPE and choroid. This method for retinal reattachment repair without tamponade then was validated in the lensectomy and vitrectomy rabbit retinal detachment model.

Methods

All procedures were performed based on the provisions of the Australian National Health and Medical Research Council code of practice for the care and use of animals in research. They were approved by the St. Vincent Hospital Animal Ethics Committee (identifier: 17-371AC). Human donor eyes were donated from the Centre for Eye Research Australia Lions Eye Donation Service, and the procedures were approved by The Royal Victorian Eye and Ear Hospital (identifier: 13-1151H-007). Research on human donor tissue adhered to the tenets of the Declaration of Helsinki.

Ex Vivo Retinal Detachment Model

Our ex vivo porcine model used freshly harvested abattoir-sourced porcine eyes (Diamond Valley, Laverton, Australia) maintained on ice for no more than 5 hours before use. In addition, human donor retinae were obtained from the Lions Eye Donation Service (Centre for Eye Research, East Melbourne, Australia) and used to validate the findings from porcine eyes. Human donor retina was retrieved and used for ex vivo experiment within 24 to 48 hours after death. Porcine eyes were prepared by removing the anterior segment just behind the limbus using a scalpel blade followed by the lens and then gentle aspiration of the vitreous using a 1-ml syringe (Terumo). The anterior segment already had been removed from human donor eyes. Four relaxing cuts then were made in the sclera, and the eyecup was flattened. Any remaining vitreous was removed using a sponge tip (Weck-Cel, BVI Medical). Using surgical scalpels (no. 22 Swann-Morton), we prepared 6 × 12-mm fresh tissue blocks (Fig 1). Using cyanoacrylate glue (Loctite; Henkel Corporation), we secured the scleral surface of the tissue block to a plastic weigh tray (ProSciTech), which then was placed under a dissection microscope (Stemi 1000; Zeiss).

We treated one of the shorter edges (6 mm) of this tissue block to mimic repair of a retinal tear margin. The immediate integrity of the repair can be examined in several ways: (1) by introducing water under the retina to test if the seal is waterproof and (2) pulling the retina tangentially and perpendicularly using a motorized micromanipulator (Zeiss) to test adhesion strength. A tangential pull mimics the effect of the weight of the retina being pulled down by gravity on the tear repair margin or surface membrane contraction. Sample sizes of 5 repeats allow us to detect differences in retinal adhesion of 0.3 g, with statistical power of 85%.

Specific Treatment Conditions

The control condition consisted of no treatment, with tissue block allowed to rest for 3 minutes in ambient conditions (humidity of 45%–50% and temperature between 20° and 22° C [XC4520 DHT11 Temperature and Humidity Sensor; Aosong Electronics Co Ltd]) before adhesion testing. In this condition, when the retina was pulled perpendicularly, the force represented the weight of the

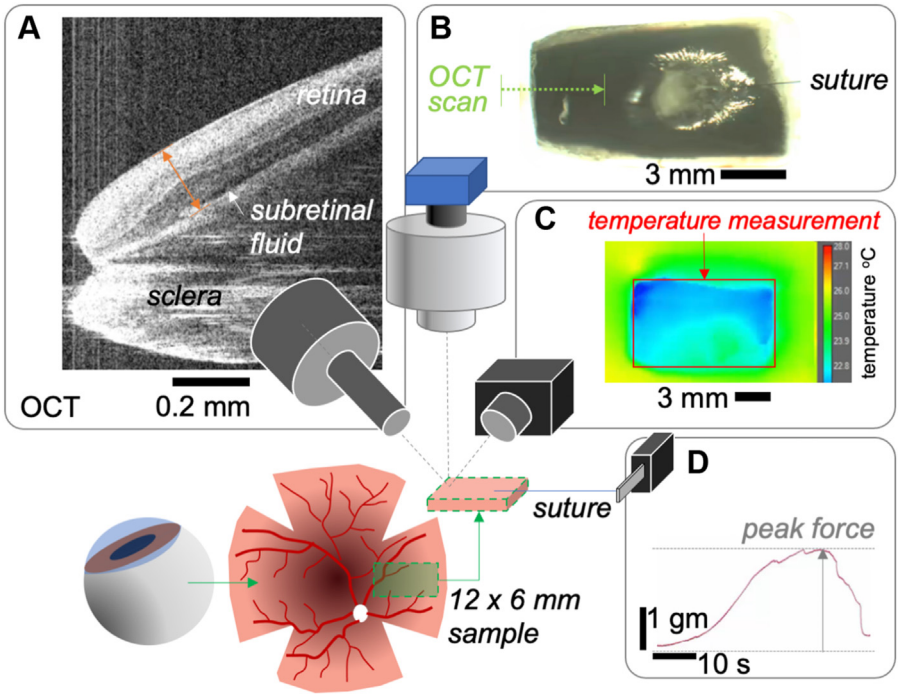

Figure 1. Ex vivo model of retinal detachment. Experimental setup to assess retinal temperature, retinal thickness, and adhesion strength between retina and the retinal pigmented epithelium (RPE) after retinal thermofusion (RTF; dehydration, then laser photocoagulation). A 6 × 12-mm section of retina with RPE, choroid, and sclera in porcine and human cadaver eyes served as an ex vivo model of retinal detachment. **A**–**C**, The retinal sample was imaged using (**A**) OCT, (**B**) color microscopy, and (**C**) a thermal camera simultaneously. The left edge of the retina was treated with RTF and pulled from the underlying RPE and choroid via an 8-0 suture attached to the retinal surface. **D**, Graph showing the maximum force required to detach the retina completely that was recorded using a force transducer, which allows quantification of the adhesion strength produced by RTF.

retina (and glue), as well as the bond between the retina and RPE. Resistance to tangential pulling represents the adhesion between the photoreceptor outer segments and the RPE. Because the tangential force is more clinically relevant, we used that as our retinal adhesion parameter, as did the methods of Zauberman[6] in the cat and those of Yoon and Marmor in the rabbit.[7]

Photocoagulation Alone. To model the current clinical approach, we compared the control condition with laser photocoagulation alone. In this case, excess fluid was wicked away from the edge of the retina using a Weck-Cell sponge point. After wicking, the 6-mm edge of the tissue block underwent standard laser photocoagulation. This was achieved by applying the retina edge laser burns using either an 810-nm (300 mW, 200 ms; Oculight SLx [Iridex]) or a 532-nm laser (200 mW power, 200 ms; Oculight TX [Iridex]) through an 25-gauge endoprobe (model no. 14120, standard straight; Iridex). Between 60 and 80 burns were applied in 2 overlapping rows along the distal 6-mm edge of the tissue block to model in vivo repair of a retinal tear. Immediately after laser application, approximately 200 µl of normal saline was added slowly under the retina around the nonlasered edges to minimize drag resulting from drying and compression by the scalpel incision. The retina then was pulled to test retinal adhesion strength, as detailed below.

Warm Air Retinal Thermofusion: The RTF approach was modeled first by dehydrating the edge of the tissue block for 1 to 3 minutes using 2 approaches. The first approach used a custom-made device to deliver heated air (30°−75° C) at flow rates of 50 to 70 ml/minute through a custom-made 25-gauge intraocular thin-walled flute (Ingeneus Pty Ltd). Under a microscope, the handheld probe was manipulated manually to maintain the tip of the flute at approximately 1 to 3 mm from the surface of the retina. The probe was moved such that the edge of the retina was dried gradually (Supplemental Video 1). Comparisons of adhesion strength were made for 1, 2, or 3 minutes of warm air dehydration alone. Additionally, adhesion strength was quantified for 2 or 3 minutes of warm-air dehydration followed by photocoagulation using an 810-nm laser, as described above. The relationship between adhesion force and temperature integral above basal tissue temperature (22.3° ± 0.4° C; T420 [FLIR]) before photocoagulation was quantified. For both the control and no dehydration conditions, this integral was close to zero.

Laser-Based Retinal Thermofusion. Because a stream of air exiting the end of a narrow tube undergoes significant adiabatic expansion, a wide area of tissue can be affected, depending on the size of the tube and the speed of airflow. Thermodynamic modeling of 50 ml/minute airflow through a 25-gauge probe will impact a retina area some 5 mm in diameter (Supplemental Fig S1A). This approach has the potential to dry the retina away from the immediate region of the retinal tear. This was confirmed using thermal imaging in ex vivo porcine tissue (Supplemental Fig S1B). To achieve more focal dehydration of SRF, we explored the possibility of harnessing the physical properties of water whereby photons are absorbed directly to energize and disrupt water molecule bonds to liberate water molecules from the liquid phase. To achieve this, we used lasers at wavelengths strongly and selectively absorbed by water to achieve more focal dehydration of retinal fluid. The absorbance spectra for water is shown in Supplemental Figure S2A, with distinct peaks at 1470 and 1940 nm.[20] We showed using 20-µl distilled water drops on glass slides that laser dehydration (using the 1470-nm laser) was

more effective than airflow alone at removing water (Supplemental Fig S2B vs Fig S2C). Laser-liberated water can reform as small droplets near the main drop (Supplemental Fig S2C). We also showed that water was dehydrated more efficiently when the dehydration laser was combined with gentle airflow. This effect was dependent on the speed of airflow (Supplemental Fig S2D, E). Thereafter, SRF dehydration was achieved using targeted laser initially at 1470 nm (Anritsu) mounted on a custom optical setup (MOGLabs) incorporating a diode-aiming laser allowing coupling to a handheld 23-gauge dual function endoprobe (23-gauge soft-tip aspirating laser probe BL5293ASP; Bausch and Lomb) so that the aspirating channel could be used for coaxial airflow to disperse the liberated water efficiently. The 1470-nm laser was superseded by a 1940-nm laser (high-power diode; Akela Laser) that was absorbed by water more strongly and showed a greater range, offering the potential to generate sufficient power for photocoagulation, not just photodehydration. For that prototype, the 1940-nm laser diode was incorporated into an existing laser chassis (eyeLase532; Ingeneus Pty Ltd) for power supply, the helium-neon laser aiming low-power visible red laser and output controls together with the fiberoptic (BL5293ASP) coupling. To optimize the power delivery to the eye further, a novel intraocular 25-gauge dual-bore handpiece (Ingeneus Pty Ltd) was constructed using low-hydroxyl fiber for improved photon transmission efficiency.

Laser power was calibrated using a power meter (PM100D; Thorlabs) attached to either an S132C (700−1800 nm) or S148C (1200−2500 nm) sensor (Thorlabs). The 1470-nm and 1940-nm lasers were used to dry SRF at a power range of 15 to 45 mW and 5 to 15 mW, respectively. Immediately after dehydration, the margin of the retinal tear underwent photocoagulation using the 532-nm laser as described above. In addition, we considered whether the 1940-nm laser when used at a higher power also could be used as a photocoagulation laser. Thus, in several samples, 1940-nm laser photodehydration was followed by 1940-nm photocoagulation (45−60 mW). We compared retinal adhesion achieved with this combination (1940-nm drying and coagulation) against 1940-nm laser photodehydration followed by 532-nm photocoagulation.

Ex Vivo Model Outcome Measures

Testing Retinal Adhesion Strength. Using a small drop of cyanoacrylate glue (Loctite), the tip of an 8-0 suture (Vicryl Ethicon; Johnson & Johnson) was attached to the surface of the retina, away from the retinal edge so as not to alter the retinal integrity, as shown in Figure 1B. The other end of the suture was attached to an isometric force transducer (MLT0402; ADInstruments) connected via a preamplifier (FE232; ADInstruments) to a data acquisition system (Powerlab 8/SP; ADInstruments) with associated software (Chart; ADInstruments). The force transducer (MLT0402) was attached to a motorized micromanipulator (Zeiss) that allowed the attached suture and retina to be pulled laterally (to the right) away from the repair edge at a rate of 0.1 mm/second (Supplemental Video 2). This allowed us to quantify any increase in force from retinal adhesion to the underlying RPE and choroid after retinal treatment. Force data (100 samples/second) were analyzed (Chart; ADInstruments) by taking the peak force achieved during the controlled pull. The difference in peak force between experimental manipulations was compared.

Ex Vivo Imaging and Analysis. A color camera (XiQ; Ximea) was used to capture a video of the tissue surface throughout the experiment (Fig 1B). The tissue block also was imaged continuously using a thermal camera (T420; FLIR) with a macro lens attached that allowed us to quantify tissue temperature throughout the experiment (Fig 1C) as soon as the accuracy of the tissue temperature measurement using thermal imaging was confirmed by placing an implantable thermocouple probe (MLT1402 T-type fast thermocouple; ADInstruments) placed under the edge of the retina. Thereafter, thermal imaging was used in preference because the thermocouple was unstable under the retinal sample and caused unwanted tissue distortion. Video sequences were acquired at a frame rate of 30 Hz and subsequently analyzed using FLIR tools to return the peak temperature and temperature integral. Temperature integral was determined by quantifying the peak basal temperature across the 6 × 12-mm retinal block. This basal temperature was averaged over 1 minute before any manipulation. The difference at more than basal temperature was quantified for each second and then summed over the full duration of retina dehydration (sum degrees Celsius × seconds). The relationship between tissue temperature integral during dehydration (i.e., before photocoagulation) and peak adhesion force was examined.

Quantifying Change in Tissue Thickness. Finally, the left most (distal) edge of the tissue block also was imaged using OCT (Bioptigen with 18-mm lens attached; Leica), as shown in Figure 1A, B (scan direction). This enabled us to quantify change in tissue thickness and SRT. Imaging (5 frames/second) was undertaken with a 3-mm B-scan (500 A-scans) oriented from left to right. This scan positioning captured the edge of the retina, the underlying RPE and sclera, the fluid meniscus, and any SRF, as shown in Figure 1A. Analysis was undertaken by measuring tissue thickness for the inner limiting membrane to the RPE. Measurements were made perpendicular to the RPE every 20 μm from the edge of the retina and at every 15 seconds from the onset of dehydration. To consider the effect of dehydration, thickness measurements for a given sample were expressed as a percentage relative to its own baseline thickness.

In Vivo Rabbit Model of Retinal Detachment

Twenty pigmented, Dutch Belt adult rabbits weighing at least 3 kg underwent the full surgical sequence in this study. First, the 1470-nm laser with airflow was used for drying the retinal tissue, and the 532-nm laser was used for photocoagulation (6 animals). This was replaced with the longer wavelength 1940-nm laser (5 animals), and finally, the 1940-nm laser was used for both drying and photocoagulation of the retina (6 animals).

Animals were premedicated via an intramuscular injection with a nonsteroidal anti-inflammatory agent (Caprieve at 1.5 mg/kg final dose; Norbrook) 15 minutes before anesthesia, at which time pupils were dilated using 1 drop of atropine 1% (Alcon), tropicamide 1% (Alcon), and phenylephrine 10% (Alcon). Induction of anesthesia was undertaken via an intramuscular injection of a combination of ketamine (35 mg/kg; Troy Laboratories) and xylazine (5 mg/kg; Troy Laboratories). Animals then were maintained using 1% to 1.5% isoflurane (Isoflo; Zoetis) delivered with oxygen at a flow rate of 2 ml/minute. Depth of anesthesia was ensured before surgery. Pulse, respiration, and anesthesia depth were monitored throughout surgery.

Surgical Technique. The key steps related to model induction are summarized in Figure 2. In brief, rabbits were positioned on their right side on a warming pad under the operating microscope, and a lid speculum was inserted. To prevent dislocation of the speculum, a 3-0 silk suture (Johnson & Johnson) was passed through the superior and inferior eyelids to secure the arms of the speculum, and the nictitating membrane also was sutured to prevent migration during surgery. Localized conjunctival peritomies were created and a 25-gauge cannula (Alcon Constellation System; Alcon) was secured with 8-0 Vicryl (Johnson & Johnson) to the sclera for the infusion. Without securing the cannula, the weight of the infusion line can dislodge

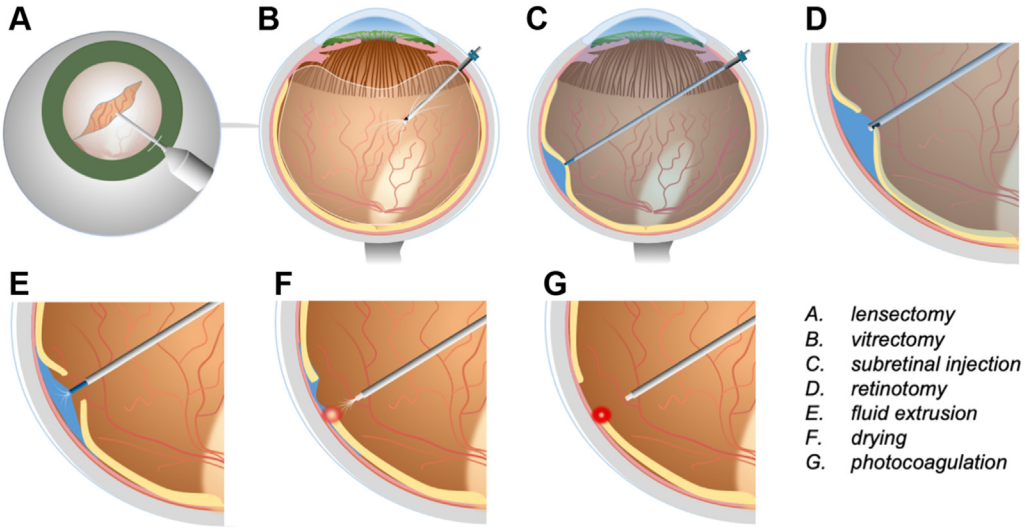

Figure 2. Schematic diagram showing in vivo induction of rhegmatogenous retinal detachment and its repair with retinal thermofusion in rabbits. After (**A**) lensectomy and (**B**) vitrectomy, retinal detachment was induced by subretinal injection of (**C**) normal saline and (**D**) retinotomy. **E**, Fluid–gas exchange was performed, and excessive subretinal fluid was extruded before repair. The tear margin was treated further (**F**) with 1940-nm laser photodehydration in continuous mode to eliminate the subretinal fluid meniscus, which (**G**) facilitates an instant sealing after 1940-nm photocoagulation. Supplemental Video 3 is a video representation of the surgery.

the cannula because the rabbit sclera is much thinner than that in human eyes, for which the cannula system was designed. The rabbit eye has virtually no pars plana for safe placement of the sclerotomies to avoid the peripheral retina, and in several preliminary surgeries, a peripheral retinal defect developed because of the fragmatome ultrasonic action resulting in retinal detachment. Thus, a near perpendicular translimbal insertion of the 25-gauge cannula through the iris root into the vitreous cavity was adopted. Adrenaline (1 μg/ml final concentration; Aspen Medicals) and low-molecular weight heparin (Enoxaparin 20 units/ml; Sanofi-Aventis) was added to the balanced salt solution (BSS; Alcon) intraocular infusion. The heparin minimizes fibrin formation,[5,21] and the adrenalin both aids stable pupil dilation and also helps to reduce any heparin-induced bleeding.

A lensectomy was essential for adequate clearance of the anterior vitreous to allow placement of the detachment bleb anteriorly so that it was high enough to remain above any pooling fluid during the dehydration phase of the retinopexy and also to avoid the teardrop effect from residual vitreous on the posterior lens capsule after the fluid–gas exchange, preventing visualization of the retinal defect margin to enable the RTF treatment to be performed. A limbal clear corneal incision was made (Clearcut S keratome blade; Alcon) to perform the 25-gauge phacoemulsification lensectomy (Infinity Ozil; Alcon). After completion of the lensectomy, a 10-0 monofilament nylon suture (Johnson & Johnson) was used to close the corneal wound. Two more 25-gauge trocars with cannulas were passed through the iris root into the vitreous cavity in the superior quadrants, and the cannulas were secured to the sclera using 8-0 Vicryl sutures.

For visualization of the retina, a Landers widefield vitrectomy system supporting arm was attached to the operating microscope, and a Peyman–Wessels–Landers lens (Ocular Instruments) was placed above the cornea. The 25-gauge vitrector and light pipe were inserted, any residual lens capsule was cleared, and then all accessible vitreous gel was removed. To ensure that as much gel as possible was removed, triamcinolone acetonide 0.1 ml (Kenacort-40; Aspen Medical) was injected repeatedly into the vitreous cavity to aid visualization of the clear vitreous[22] and to ensure as complete a removal of vitreous as possible. The vitreous was attached more firmly over the medullary wing than elsewhere, and the peripheral vitreous fibrillar density was much less in the periphery, consistent with previous anatomic studies.[23] An attempt to create a posterior detachment was made in all cases but not completely convincingly in all cases in this rabbit model. In one case, a small retinal tear developed at the border of the medullary rays, causing a localized detachment, and surgery was abandoned. When no obvious release had occurred (as seen in human surgery) after multiple high-vacuum aspiration attempts, high-vacuum aspiration was performed extensively after repeat triamcinolone acetonide injection over wide areas of the peripheral retina. No difference was found in the postoperative course of those animals with no intraoperative tears.

To create the retinal detachment, BSS (Alcon) was injected into the SRS through a soft-tipped 25-gauge cannula (Alcon) attached to a syringe controlled by an assistant. The soft-tipped cannula was placed on the retinal surface as the BSS injection commenced, and the injection was maintained until an adequate area of detachment formed. The localized bleb of retinal detachment was created as anteriorly as possible in the mid periphery of the inferior retina so that it remained above any reaccumulating fluid and could be kept dry. The vitrector was used to create a retinal defect (2–3 mm in diameter) to mimic retinal tears found during retinal detachment surgery. A standard fluid–gas exchange with aspirating 25-gauge soft-tipped cannula through the retinal defect was performed, as in traditional vitreoretinal surgery.

As soon as the retinal tear margin and the retina were reattached, according to routine surgical criteria, dehydration of a 1- to 2-mm retinal zone around the tear margin was achieved with the combination of laser (initially with the 1470-nm prototype and subsequently with the 1940-nm unit) and an airstream delivered via the aspirating channel of a 25-gauge aspirating laser handpiece (25-gauge soft-tip aspirating laser probe BL5293ASP) with the aid of an aiming beam. The airflow was generated by an independent syringe pump (22; Harvard Apparatus) connected through a fine syringe filter (0.22 μm; Millex GV, Merck Millipore). The airflow was controlled between 20 and 40 ml/minute by the assistant. The

intraocular pressure was not affected because of the regulation of intraocular pressure by the Constellation console vented gas forced infusion control system. The laser for photodehydration was used at power of 15 to 45 mW for the 1470-nm laser and 5 to 15 mW for the 1940-nm laser, and drying took between 3 and 5 minutes. Adequate dehydration was judged when the sheen from the fluid meniscus where the retinal margin joined the exposed RPE layer was lost, the adjacent retinal surface developed a matte reflex, and the dehydrated retina appeared darker and thinner than the adjacent untreated retina.

Because of the formation of copious plasmoid aqueous by the rabbit eye,[24] the retinal defect was sometimes flooded by this fluid, thus preventing SRS dehydration. In addition, sometimes the laser probe became adherent to it, and movement displaced the retinal edge. To counter this, we modified our technique to incorporate a chandelier fiberoptic light (25-gauge; W/RFID 8065751577 [Alcon]) so that, with a bimanual technique, concurrent continuous aspiration (25-gauge soft tip) within the retinal tear was performed during the laser dehydration and subsequent photocoagulation.

As soon as adequate dehydration was achieved, 2 to 3 continuous rows of 500-ms duration laser pulses using a 532-nm (Iridex) laser with a spot size of approximately 500 μm set at a duration of 500 ms delivered via a 25-gauge laser fiberoptic (BL5293ASP) was applied around the tear margin. The intensity was set at levels sufficient to produce opacification of the treated retina (150−250 mW, pulsed). A similar effect could be achieved using the 1940-nm laser set at higher power (45−60 mW, continuous). In 3 rabbits (1 that received laser treatment only and 2 that had undergone the RTF procedure) 10-0 sutures secured to the retina below the inferior tear margin using fibrin glue (Fibrin Sealant; Baxter). As above, this suture was attached to an isometric force transducer (MLT0402), and using a motorized micromanipulator (Zeiss), constant force was applied over 90 to 120 seconds to test adhesion strength. Animals were killed at the end of the adhesion test.

In the remaining 17 rabbits, BSS infusion then was recommenced slowly to fill the vitreous cavity. The sclerotomies were closed with a 10-0 nylon monofilament suture (Ethicon; Johnson & Johnson), and exposed cut suture ends were rounded off using the 532-nm laser to soften the cut ends. These animals were followed up for 14 days.

After surgery, animals received 5 ml of warmed Hartman's solution subcutaneously (Baxter) and were kept warm until they regained the righting reflex. After awakening and over the first day, animals were encouraged to drink (hand fed using a 50-ml syringe if necessary) and to eat softened food pellets. Postsurgical care of eyes consisted of mydriatic (1% atropine once daily; Alcon), Prednefrin Forte 4 times daily (Allergan), and antibiotic ointment 4 times daily (1% Chlorsig; Aspen Pharma). Additional subcutaneous warmed Hartman's solution was given if any signs of dehydration were present. Caprieve (Norbrook) was given once daily if animals showed any signs of pain.

Two weeks after surgery, animals were deeply anesthetized (intramuscular ketamine 35 mg/kg and xylazine 5 mg/kg mixture), and images of the retina were obtained using a fundus camera (Micron III; Pheonix). Immediately after imaging, animals were killed (intravenous 100 mg/kg Lethabarb; Virbac). After eyes were enucleated, 100 μl of Davidsons's fixative was injected into the eye using a 30-gauge needle through the cornea. The eye then was immersed in Davidson's fixative for between 16 and 24 hours. Eyes then were dissected and processed for paraffin embedding (Melbourne Histology Platform, Parkville, Australia). Ten-micron thick sections were cut through the treated area and stained with hematoxylin−eosin (Sigma). Images were captured using ×2 0.05 NA or ×10 0.40 NA objective on an BX51 brightfield microscope (Olympus) at the Microscope Facility at The Florey Institute of Neuroscience and Mental (Melbourne, Victoria, Australia). Outcome measures were in vivo fundus imaging and histologic confirmation that the retinal repair remained intact after 14 days.

Statistical Analyses. Data are given as group mean ± standard error of the mean. Comparisons between conditions were made using the 1-way analysis of variance [ANOVA], with Dunnett's multiple comparisons between groups (Prism 9; GraphPad).

Results

Ex Vivo Retinal Detachment Model

Figure 3 shows that warm air (50°−70° C) at rates between 20 and 70 ml/minute changes the appearance of ex vivo porcine retina on OCT. After 3 minutes of dehydration, less evidence of SRF, retinal thinning, and increased reflectivity was observed at the level of the RPE and inner limiting membrane, and overall, a more homogenous retinal appearance was observed. Quantification of retinal thickness at the edge of the repair confirmed that the largest effect occurred nearest the retinal margin. Overall, the retina was significantly thinned ($P < 0.001$, time effect on 2-way ANOVA), specifically by 16 ± 3% after 3 minutes.

Next, we considered the effect of RTF on adhesion achieved between the retina and underlying RPE and choroid (Fig 4A). After treatment, on the left edge of the retinal section, cyanoacrylate glue was applied near the midpoint of the retina, and a fiber connecting the retina to the force transducer was attached (Fig 4A). Figure 4B shows an example of force traces during a controlled pull toward the right, away from the retinal repair edge. Compared with photocoagulation alone, RTF using warmed air dehydration before photocoagulation using an 810-nm laser produced higher adhesion force (Fig 4B). Note that forces of > 2 *g* often (approximately 80% of cases) exceeded the strength of the postmortem porcine retina. Such forces resulted in the untreated retina tearing from the RTF-treated zone. The peak force in those instances thus underestimated the separation force of the RTF bond itself. Because of the nature of cyanoacrylate chain polymerization (exothermic and can release formaldehyde[25,26]), gluing a fiber over the thermofusion bond area distorts the retinal strength; as such, no attempts were made to measure the attachment strength directly. Nevertheless, the peak force was used here as a surrogate for repair adhesion strength, as summarized in Figure 4C. Photocoagulation alone did not increase adhesion significantly compared with untreated samples ($P = 0.98$, 1-way ANOVA with multiple comparisons). Dehydration for 2 or 3 minutes (1 minute, $P = 0.86$; 2 minutes, $P = 0.01$; 3 minutes, $P = 0.0008$) and RTF with dehydration for 2 minutes ($P = 0.0016$) or 3 minutes ($P < 0.0001$) all produced significantly higher adhesion. Figure 4D shows that the strength of adhesion increased with higher temperature integrals achieved during the dehydration process, with data for dehydration alone, as well as for RTF (drying followed by photocoagulation), both following a similar relationship. Although the warm air achieved SRF

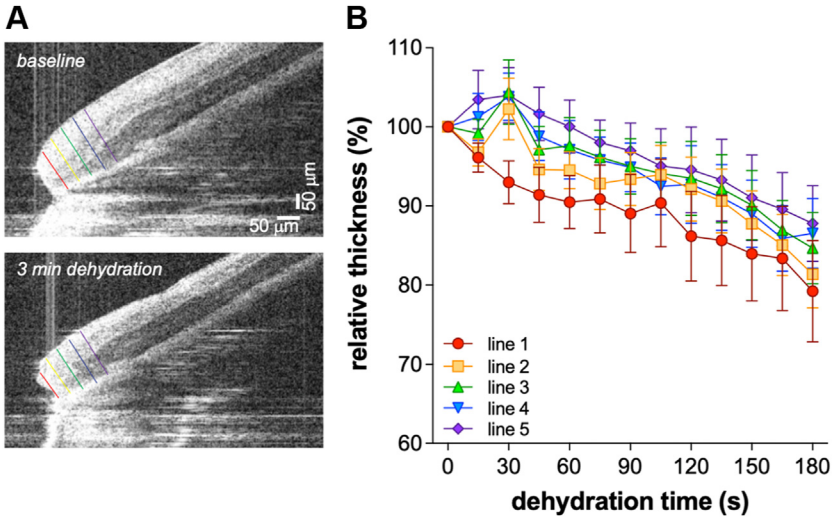

Figure 3. Effect of warm air dehydration on retinal thickness. **A**, Representative OCT images before and after 3 minutes of dehydration. Total retinal thickness at the edge treated by warm airflow was determined at 5 locations, each 50 µm from the edge of the retinal margin. **B**, Graph showing gradual reduction of retinal thickness over the course of dehydration (n = 15). Error bars are standard error of means. Measurement lines are color coded in (**B**) as per (**A**).

dehydration and facilitated strong bond formation (Fig 4), the thermal footprint of warm air dehydration was much greater than the diameter of the delivering tube because of adiabatic expansion of moving air out of a small aperture (Supplemental Fig S1A, B) and has the potential to damage the retina well beyond the immediate zone of

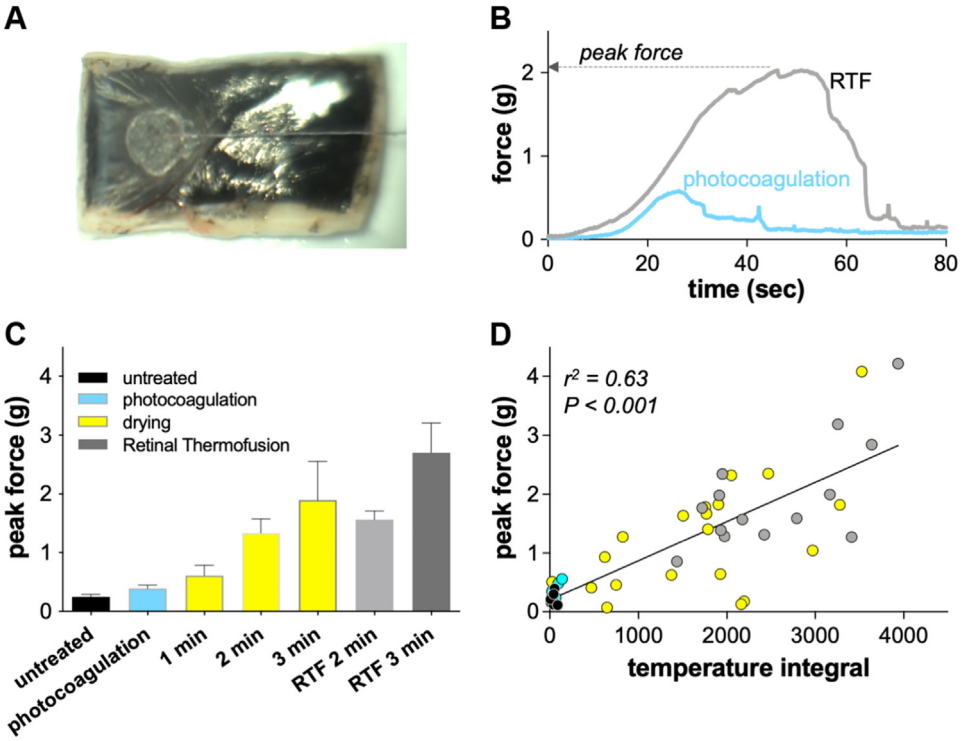

Figure 4. Adhesion strength of retinal thermofusion in ex vivo porcine eyes. **A**, After treatment, cyanoacrylate glue was applied, and a fiber connecting the retina to the force transducer was attached. Photograph showing a micromanipulator pulling at a constant rate, causing the stress lines between the dried glue and the RTF-treated retinal edge. **B**, Line graph showing force traces for 2 samples in which the peak adhesion force was higher as a result of retinal thermofusion (RTF; gray trace) than laser coagulation alone (blue trace). **C**, Bar graph showing peak force measured for untreated (n = 9), photocoagulation alone (n = 5), warm air drying (1 minute, n = 6; 2 minutes, n = 9; and 3 minutes, n = 5), and RTF (n = 5). Stronger adhesion was achieved with RTF than with warm air drying and photocoagulation alone. **D**, Scatterplot showing that the peak force achieved was associated with the temperature-time integral of drying before photocoagulation. Error bars are standard error of means. Figure legend in (**D**) is as per (**C**).

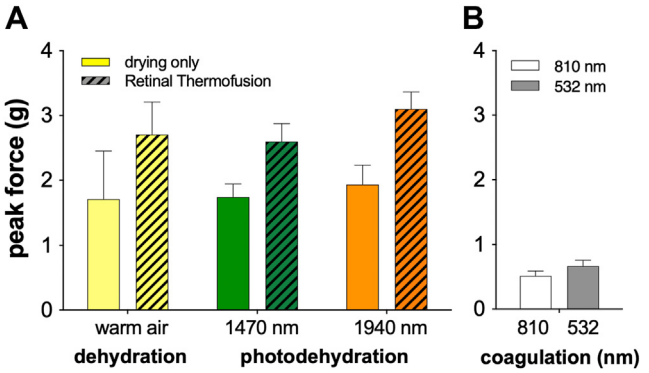

Figure 5. Bar graphs showing a comparison of retinal thermofusion achieved with warm air dehydration or laser photodehydration. **A**, Using the ex vivo porcine retina preparation, similar levels of adhesion force were achieved when dehydrating for 3 minutes with warm air (n = 5), 1470-nm laser (n = 6), or 1940-nm laser (n = 4). Higher force was achieved when dehydration was followed with photocoagulation (warm air dehydration followed by 810-nm laser photocoagulation [n = 5], 1470-nm photodehydration [n = 13], and 1940-nm photodehydration [n = 14] followed by 532-nm photocoagulation). **B**, Retinal adhesion force achieved was similar between 810-nm (n = 8) and 532-nm (n = 11) photocoagulation laser. Error bars are standard error of means.

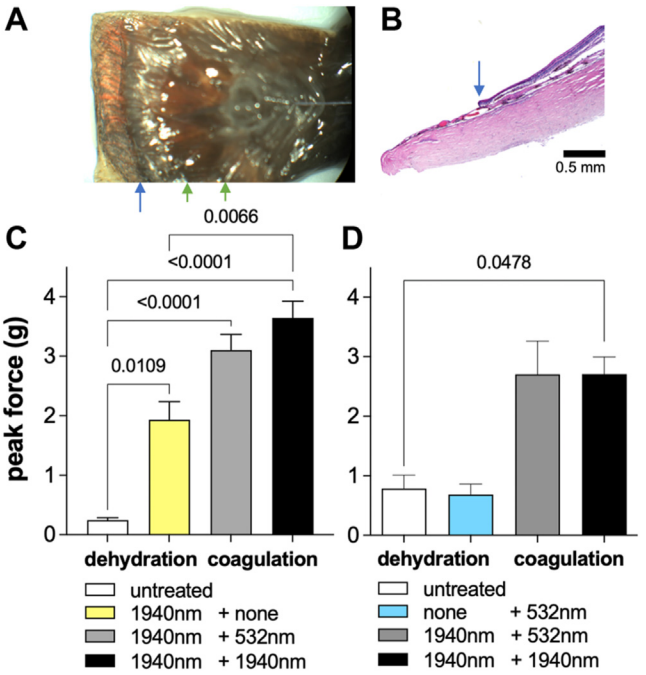

Figure 6. Effectiveness of photodehydration followed by 532-nm or 1940-nm laser photocoagulation in ex vivo porcine and human retina. **A**, Photograph showing donor tissue with model retinal tear to the left. Margin of dehydration and repair indicated by the blue arrow. The green arrows indicate margins of a new retinal tear induced by a tangential pull. The retina was bunched to the right of the cyanoacrylate glue. **B**, Photomicrograph (original magnification ×2) showing hematoxylin–eosin staining of a retinal cross section showing bonding of the retina to the retinal pigment epithelium and choroid. **C**, Bar graph showing that photodehydration of porcine tissue produced higher adhesion force (group sizes: untreated, n = 9; 1940-nm dehydration, n = 4; 1940-nm dehydration and 532-nm photocoagulation, n = 14; and 1940-nm dehydration and photocoagulation, n = 12). **D**, Bar graph showing that photodehydration followed by photocoagulation produced significantly higher adhesion (group sizes: untreated, n = 4; 532-nm photocoagulation, n = 4; 1940-nm dehydration and 532-nm photocoagulation, n = 7; and 1940-nm dehydration and photocoagulation, n = 10).

dehydration. This is clinically unacceptable. A novel approach to dehydrating the SRS that limits the thermal footprint (Supplemental Fig S1C) is to use lasers tuned to wavelengths targeting key water absorption peaks (Supplemental Fig S2A). Supplemental Figure S2 also shows that more effective dehydration was achieved when laser dehydration was used in combination with airflow (Supplemental Fig S1D, E).

Figure 5A shows that, when used in combination with low airflow (20 ml/minute), dehydration using 1470-nm or 1970-nm lasers produced similar retinal adhesion forces ($P = 0.95$, 1-way ANOVA). When dehydration was followed by photocoagulation, retinal adhesion force consistently was higher than with laser dehydration alone ($P = 0.92$ for interaction, $P = 0.64$ type of treatment, and $P = 0.0045$ for photocoagulation effect, 2-way ANOVA). Because some early experiments used 810-nm photocoagulation (because of the availability of that laser in the laboratory), whereas later experiments used 532-nm photocoagulation, we compared these directly. Figure 5B shows that the 810-nm and 532-nm laser photocoagulation bonding effects were not different ($P = 0.24$, t test) and thus can be used interchangeably for photocoagulation.

As soon as we had established the ex vivo retinal detachment model, we wanted to ensure that our observations on porcine specimens also were relevant to human retina tissue. We quantified adhesion force achieved using the 1940-nm laser for tissue photodehydration followed by 532-nm or 1940-nm laser photocoagulation in porcine or human retinal samples (Fig 6B, C, respectively). Photodehydration alone produced greater adhesion strength than controls (Fig 6C). Retinal thermofusion produced stronger adhesion than drying alone. In human tissues, RTF resulted in significantly stronger adhesion than untreated samples (Fig 6D). Comparisons of photocoagulating lasers showed that, for both porcine (Fig 6C; $P = 0.49$) and human (Fig 6D; $P = 0.99$) tissue, no difference was found between the 532-nm and 1940-nm lasers that were applied after 1940-nm drying.

In 3 rabbits, we assessed retinal adhesion strength in vivo. Gluing the suture to the retinal tear margin proved to be particularly challenging because cyanoacrylate released formaldehyde,[27] causing corneal opacification. After some trial and error, we were successful when the cyanoacrylate was replaced with a fibrin glue that produces a natural adhesive, relying on the formation of a fibrin clot to hold the suture firmly in place. Figure 7A shows 3 adhesion force traces obtained from RTF using a 1470-nm laser for photodehydration and a 532-nm laser for coagulation. The force required to pull the retina away

from the choroid was > 2 *g*, which was greater than the ex vivo baseline force of 0.5 *g* (Fig 7A).

Clinically, the strength of retinal adhesion is in itself not important (formation of an effective waterproof seal is the priority) for most cases during retinal detachment repair, but retinal slippage during GRT repair remains a significant surgical challenge,[28] despite the introduction of perfluorinated liquids (PFCLs) to reposition the retina. To assess whether the RTF method could prevent GRT slippage in a PFCL-filled eye, we first measured ex vivo the transmission of 1940-nm light through a PFCL (Oktaline perfluoro-octane liquid; Bausch and Lomb) and showed that, whereas water allowed 1.1 ± 0.9% transmission, PFCL allowed 87% transmission of the 1940-nm laser. We then created a GRT model by placing a 6 × 12-mm strip of porcine retina inside a well (Supplemental Fig S4A) to hold the tissue block vertically, after which a microfiber was glued to the retinal surface (as per the previous testing). When compared with an untreated upper retinal edge, RTF either in air or with the laser probe and retinal block submerged both produced significant increases in adhesion force (Supplemental Fig S4B; $P = 0.04$, 1-way ANOVA). No difference was found between the 2 approaches in terms of resultant force ($P = 0.42$, post hoc test).

Longer-term Surgery Outcome of RTF Repair in a Rabbit Model

Initially, we used the 1470-nm laser for drying followed by the standard 532-nm clinical laser for photocoagulation (6 surgeries). The 1940-nm laser subsequently replaced the 1470-nm laser for drying, and then the procedure was refined further to using the same laser at 1940 nm for both tissue photodehydration and coagulation in the final surgical protocol. Animals were monitored for at least 2 weeks after surgery, at which point fundus photographs were used to assess whether the retina remained intact before enucleating the eye for histologic processing and further confirmation. Figure 7B summarizes uncomplicated, completed surgeries for the different surgical approaches. For 1470-nm laser photodehydration followed by 532-nm laser photocoagulation, 4 retinal repairs remained attached; however, in 2 surgeries, retinae were detached at the end point. For RTF surgery using the 1940-nm laser for photodehydration followed by coagulation using 532-nm or 1940-nm lasers, repair was successful in all cases at the end point, as determined by fundus imaging and histologic analysis (Fig 8 is representative of 2 surgeries, with remaining histologic findings in Supplemental Fig S3). Hematoxylin–eosin staining of the tissue showed an obvious loss of the retinal architecture and therefore thinning at the RTF repair site because of the thermal effect of the 1940-nm laser and, importantly, fusion of the retina to the RPE and choroid, as indicated by the lack of SRS (colored arrows), unlike the nondehydrated retina region adjacent to the site of repair. At the edge of the RTF repair site where no surgery was performed, a transition to normal retina was seen whereby retinal layers were easily distinguished. Supplemental Figure 5 suggests that this transition zone is < 1 mm.

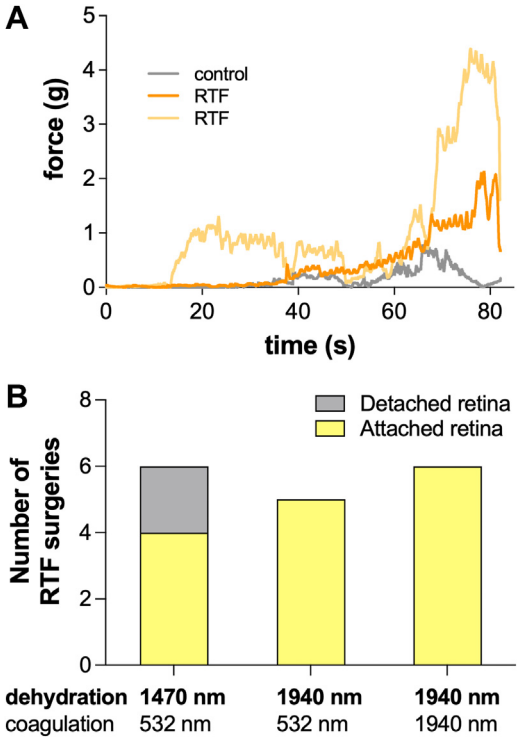

Figure 7. In vivo retinal thermofusion (RTF) in rabbit eyes. **A**, Line graph showing that, in 2 eyes, in vivo RTF produced peak forces of 2.12 *g* (orange) and 4.39 *g* (yellow) adhesion force, compared with the control (0.79 *g*, gray trace). **B**, Bar graph showing summary of completed RTF surgeries in 17 animals. All surgeries using photodehydration (either 1470 nm or 1940 nm) followed by 532-nm coagulation or 1940-nm laser for both drying and coagulation. The primary outcome was confirmation that the entire retinal tear margin was attached as confirmed by in vivo funduscopy, as well as postmortem histologic analysis. With the 1940-nm laser (followed by coagulation with either the 532-nm or the 1940-nm laser), all repairs were attached, whereas when using the 1470-nm laser for drying and 532-nm laser for coagulation, 2 of the 6 repairs had detached retinas at the end point.

Retinal thickness measurements showed no significant differences in retinal thickness for any region away from the repair edge, suggesting that gross retinal structure largely was unaffected.

Discussion

Sealing all retinal tears is the essential surgical step to treat a rhegmatogenous retinal detachment. Since Gonin developed the ignipuncture method using a thermal injury to both the retina and the adjacent RPE and choroid,[2–4] it has not been possible to cure detachments during surgery reliably without some form of support holding both injured layers together while the wound-healing process occurs. A method that is independent of a wound-healing response to create an immediate seal that is independent of the tear location would eliminate the need to support the retina with a tamponade agent, either as gas or liquid, thus restoring vision quickly, enabling earlier return to normal activities, including air

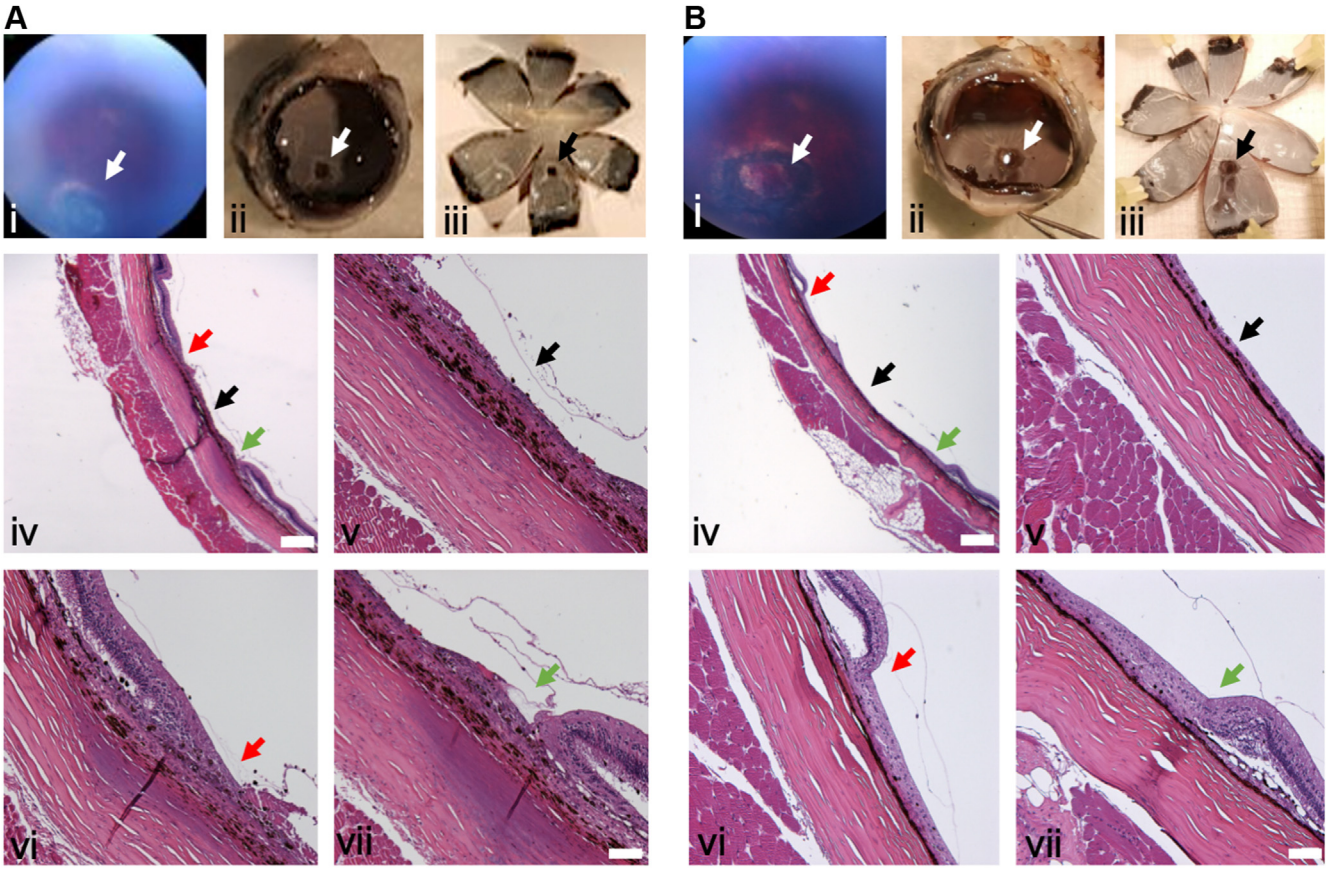

Figure 8. **A**, **B**, In vivo retinal thermofusion (RTF) repair in the rabbit model in 2 representative eyes. **Ai**, **Bi**, In vivo fundus image of the retinal tear 2 weeks after RTF repair using 1940-nm photodehydration followed by 1940-nm photocoagulation. The pigmentary reaction around the edge of the retinal tear was evident. **Aii**, **Bii**, Photographs of postmortem eyes with the anterior segment removed showing intact retina and attached retina tear margin (arrow). **Aiii**, **Biii**, Photograph showing eyecup with relaxing cuts before processing for histologic analysis, with the attached retinal tear (arrow). **Aiv**, **Biv**, Photomicrographs showing cross sections (original magnification, ×2) through the retinal tear, with the edges of the tear indicated by the red and green arrows (stain, hematoxylin–eosin). Scale bar = 200 μm. **Av–vii**, **Bv–vii**, Photomicrographs showing repaired tear margin (red and green arrows) and a region within the entire area free of overlying retina (stain, hematoxylin–eosin; original magnification, ×10). Black arrow region between repair edges = red and green arrows RTF repair site edge. Scale bar = 50 μm.

travel, much earlier, with potentially better quality of vision. After the SRS is isolated during surgery, the vitreous cavity can be refilled with BSS[29] at the end of the retinopexy, allowing the physiologic mechanisms of SRF removal[30] for retinal reattachment to occur in a similar manner to pneumatic retinopexy. This should offer similar potential benefits to pneumatic retinopexy when compared with vitrectomy: a lower risk of retinal displacement,[31–34] retinal folds,[35,36] and disruption to the outer retina as evidence by discontinuity of the ellipsoid zone and external limiting membrane, as seen with OCT.[16,37]

Consistent with a previous study,[18] we showed histologically that RTF can bond the retina and underlying RPE and choroid instantaneously in a rabbit retinal detachment model (Fig 8), producing immediate and strong adhesion of the retina to the underlying RPE and choroid. Functional demonstrations of immediate and strong adhesion also were made using ex vivo porcine tissue (Fig 4) and human tissue (Fig 6), as well as in vivo in rabbit eyes (Fig 7A). Moreover, we were able to show enduring adhesion throughout a 2-week follow-up period using the in vivo rabbit retinal detachment model.

The key clinical finding is that a short preliminary step of SRS dehydration at the retinal tear margin allows both tissues to be in contact at the time of coagulation, resulting in fusion of the retina to underlying RPE and choroid and creating an immediate and strong adhesion. Furthermore, we showed that RTF can be achieved by targeting energy absorption peaks at 1470 nm or 1940 nm to agitate and release water molecules in situ from the liquid phase to vapor. When coupled with low airflow (10–20 ml/minute), this approach was effective at removing SRF, allowing for photocoagulation to produce an immediate adhesion between the retina and underlying RPE and choroid. The addition of low airflow at room temperature increased the speed of dehydration while avoiding excessive drying of adjacent retinal areas associated with adiabatic expansion of high speed (50–70 ml/minute) warm air and prevented potential elevation of intraocular temperature that can enhance retinal damage.[38]

Retinal Attachment Force Determination

To test the efficiency of a variety of dehydration methods, we developed an ex vivo full-thickness retina−RPE−choroid−sclera model broadly based on the method of Yoon and Marmor[7] and of Zauberman.[6] Herein, we showed that the porcine eye tissue provides a robust model for human tissue, showing dehydration and coagulation characteristics, as well as adhesion forces that are comparable with those of human tissue.

Retinal adhesion to the underlying RPE and choroid was measured using the same standardized explant preparation (see "Methods"). We believe this is the first documentation of retinal adhesion strength immediately after laser photocoagulation. Yoon and Marmor[7] created a bleb of retinal detachment, allowed it to reattach spontaneously, and then treated both the reattached retina and nondetached (control) retina. They found that the attachment was only 50% of normal at 8 hours, rising to twice normal after 3 days, but they did not measure adhesion immediately after laser treatment.

Zauberman[6] assessed the adhesion strength after photocoagulation, diathermy, and cryopexy in the cat eye using a similar methodology to ours but assessed the adhesion strength between 2 and 96 days after treatment. They found that the adhesion over the tapetum lucidum ranged from 15 to 40 mg at day 2, rising to 65 to 155 mg at day 7, with a maximum of 185 to 365 mg from day 21 onward. No measurements were made immediately after the treatment.

Over the course of 3 minutes of dehydration, the retina thinned by 20% (Fig 3), with regions nearer the retinal edge showing the most thinning. The fluid meniscus at the retinal edge and exposed RPE interface also was monitored and was noteworthy because the meniscus reformed after the initial drying passes, presumably as more peripheral SRF was drawn to the exposed retinal edge. This continued until the more distal retina also had dehydrated. This phenomenon also was noted in vivo during the rabbit eye detachment surgery. Several clinical indicators proved to be reliable indirect markers of adequate SRS drying: removal of the fluid meniscus dark band at the retinal defect edge, thinning of the retinal edge creating a distinct step down from the adjacent untreated retina, loss of surface reflectivity (glistening) from the hydrated retina or RPE surface, and the development of a dull, subtly stippled sheen as the retinal surface dried. These metrics were used successfully to judge adequate dehydration before coagulation.

We showed that the immediate adhesion force achieved was related to the tissue temperature integral (temperature × time) achieved using the dehydration phase (Fig 4D), with drying for longer durations producing stronger immediate adhesion. We interpret these observations to be the result of dehydration of glycoproteins located on both retinal photoreceptors and RPE[39,40] cell membranes, thus reducing their lubrication effect.[41] Critically, this increased adhesion from drying alone could be reversed rapidly with rehydration and did not create a clinically useful retinopexy adhesion. We believe that the ready slippage of the retina during GRT repair or with macula translocation after macula detachment occurs because the SRF hydrates glycoproteins and increases their lubricious quality.

In Vivo Rabbit Eye Surgery

In vivo laser photodehydration with coaxial airflow resulted in more targeted dehydration largely confined to the laser footprint. This is because the release of water molecules from the water phase (evaporation) primarily is the result of the photons energizing the water molecular bonds. The low rate of airflow (10−20 ml/minute) helped to disperse the laser-liberated water molecules faster than without any coaxial flow (Supplemental Fig 2) without the risk of retinal edge elevation, as can occur with more forceful airflow. Importantly, no observable retinal surface dehydration was observed, nor other adverse effects beyond the laser-exposed area, in distinct contrast to the effect created by the warm air dehydration method (Supplemental Fig 1A). We believe this to be because the evaporation effect primarily is the result of the photic disruption of the water−water bonds in the liquid phase, with the airflow being just enough to disperse the vapor. As with traditional photocoagulation, slow continuous movements ("painting") around the retinal defect margin are performed for 2 to 3 minutes, during which the retinal surface at the defect edge becomes thinner and the margin appears darker (choroidal pigment was more visible through the thinner retina) and develops a matte or slightly speckled appearance to match the matte appearance of the dried, exposed RPE within the defect (Supplemental Video 4). Initially, the base of the retinal defect edge in contact with the RPE showed a persistent glistening from the fluid meniscus. Even after the meniscus is minimized, it can reform because residual SRF is recruited from the surrounding areas until prevented by sufficient retinal dehydration of the area surrounding the tear. The clinical judgment of adequate retinal dehydration before using higher power to achieve photocoagulation will be a critical skill to acquire.

It is important to recognize that evaporation of the meniscus was achieved best by aiming the laser or airflow directly at the meniscus at the RPE and retinal tear edge because the evaporation effect primarily is the photon stream. If the meniscus is in shadow, it will be underexposed to the photons and not evaporated efficiently.

The laser power output and spot size and the speed of moving the fiberoptic tip during the dehydration were monitored visually during the dehydration so that no retinal opacification occurred, which would indicate a temperature elevation toward the coagulation range. The laser beam is mildly divergent leaving the fiberoptic tip; as such, laser power density varies with the distance between handpiece tip and retina, as with a traditional 532-nm or 810-nm laser fiberoptic delivery. The 1940-nm coaxial probe we developed delivers sufficient power to coagulate the retina and RPE but uses water molecules as the chromophore rather than melanin or hemoglobin. This effect is not dependent on dehydration of the SRS so that the laser can be used—with or without the airflow—to photocoagulate other areas of retina for prophylactic laser or to treat tears in attached retina. However,

because the laser energy is absorbed by water, this wavelength cannot be used to treat the retina when delivered though the cornea or via an indirect ophthalmoscope, nor via a fiberoptic in the presence of vitreous.

The RTF method achieves at vitrectomy the effect of pneumatic retinopexy, obstructing access of liquid vitreous to the SRS but does so regardless of the tear location (and presumably the length). As such, it offers the potential to facilitate macular reattachment as the outer retinal edema is diminishing[36] and to achieve the same potential quality-of-vision benefits documented in the Pneumatic Retinopexy versus Vitrectomy for the management of Primary RRD (PIVOT) trial and reduction of the incidence of outer retinal folds.[35] One of the most important potential benefits of 1940-nm laser-based RTF is the immediate adhesion formation along a GRT before the removal of the PFCL, thus preventing retinal slippage after PFCL removal and eliminating the need for longer-term tamponade and potential second surgery.[1,42] Allowing the retina to reattach naturally via RPE pumps may result in better vision outcomes.[16,35,36]

The laser-based RTF method to encircle a retinal tear margin with laser is an intuitive manipulation for trained retinal surgeons. The purpose-built 25-gauge coaxial fiber-optic with the high transmission of near infrared light by the low-hydroxy fiber ensures that the 1 handpiece can be used for both photodehydration and photocoagulation, thus minimizing the exchange of instruments and reducing the surgery time.

Conclusions

The insertion of a short preliminary step of photodehydration before laser photocoagulation enables formation of a strong immediate attachment of the retina to the underlying RPE and choroid in the retinal detachment rabbit model. The creation of an immediate and stable intraoperative retinopexy seal should enable retinal detachment repair without tamponade, regardless of the retinal tear or relaxing retinotomy location, and should reduce the need significantly for liquid tamponade and the second procedure for its removal. Should the RTF technique prove beneficial in a clinical trial, it may be a significant step forward for the field.

Acknowledgments

The authors thank Professor Robert Scholten and Dr Sebastian Saliba, Moglabs, Carlton, Australia, for their invaluable support and expertise with laser systems.

Footnotes and Disclosures

Originally received: January 27, 2022.
Final revision: May 25, 2022.
Accepted: June 6, 2022.
Available online: June 13, 2022. Manuscript no. XOPS-D-22-00017.

[1] Retinology Institute, Glen Iris, Australia.

[2] Centre for Eye Research Australia, East Melbourne, Australia.

[3] Department of Optometry and Vision Sciences, University of Melbourne, Parkville, Australia.

[4] Caring Futures Institute, Flinders University, Bedford Park, Australia.

[5] Department of Ophthalmology, Dokkyo Medical University Saitama Medical Center, Saitama, Japan.

Disclosure(s):

All authors have completed and submitted the ICMJE disclosures form.

The author(s) have made the following disclosure(s): W.J.H.: Patent — 2014207245, 14/799,330, 2019200894, 16/270,996, 2020903130, PCT/AU2021/051020

A.B.M.: Patent — 2019200894, 16/270,996, 2020903130, PCT/AU2021/051020

M.O.: Consultant — Roche; Lecturer — Roche, Allergan, AbbVie

B.V.B.: Patent — 2019200894, 16/270,996, 2020903130, PCT/AU2021/051020

Supported by the US Department of Defense Office of the Congressionally Directed Medical Research Programs (CDMRP), under the Vision Research Program (Technology/Therapeutic Development Award no.: W81XWH-16-1-0787).

HUMAN SUBJECTS: Human donor eyes were donated from the Centre for Eye Research Australia Lions Eye Donation Service (LEDS) and their use approved by The Royal Victorian Eye and Ear Hospital Human Research Ethics Committee. Research in accordance with to the Declaration of Helsinki.

Nonhuman animals were used in a study. Protocol was approved by the St. Vincent Hospital Animal Ethics Committee. All procedures were performed based on the provisions of the Australian National Health and Medical Research Council code of practice for the care and use of animals in research.

Author Contributions:

Conception and design: Heriot, Metha, He, Okada, Bui

Analysis and interpretation: Heriot, Metha, He, Lim, Hoang, Nishimura, Okada, Bui

Data collection: Heriot, Metha, He, Lim, Hoang, Nishimura, Okada, Bui

Obtained funding: N/A; Study was performed as part of the authors' regular employment duties. No additional funding was provided.

Overall responsibility: Heriot, Metha, He, Lim, Hoang, Nishimura, Okada, Bui

Abbreviations and Acronyms:
ANOVA = analysis of variance; **BSS** = balanced salt solution; **LEDS** = Lions Eye Donation Service; **GRT** = giant retinal tear; **PFCL** = perfluorinated liquid; **RPE** = retinal pigment epithelium; **RTF** = retinal thermofusion; **SRF** = subretinal fluid; **SRS** = subretinal space.

Keywords:
Retinopexy, Tamponade, Vitrectomy, Detachment.

Correspondence:
Wilson J. Heriot, MB, BS, Centre for Eye Research Australia, Level 7/32 Gisborne Street, East Melbourne, 3002 Victoria, Australia. E-mail: wheriot@unimelb.edu.au.

References

1. Wong D, Williams RL, German MJ. Exchange of perfluorodecalin for gas or oil: a model for avoiding slippage. *Graefes Arch Clin Exp Ophthalmol*. 1998;236(3):234–237.

2. Rumpf J, Gonin Jules. Inventor of the surgical treatment for retinal detachment. *Surv Ophthalmol*. 1976;21(3):276–284.

3. Wolfensberger T, Gonin Jules. Pioneer of retinal detachment surgery. *Indian J Ophthalmol*. 2003;51(4):303−308.
4. Gonin J. La pathogénie du décollement spontané de la rétine. *Ann d'Ocullist (Paris)*. 1904;132(1):30−55.
5. Johnson R, Irvine A, Wood I. Endolaser, cryopexy, and retinal reattachment in the air-filled eye: a clinicopathologic correlation. *Arch Ophthalmol*. 1987;105(2):231−234.
6. Zauberman H. Tensile strength of chorioretinal lesions produced by photocoagulation, diathermy, and cryopexy. *Br J Ophthalmol*. 1969;53(11):749−752.
7. Yoon Y, Marmor M. Rapid enhancement of retinal adhesion by laser photocoagulation. *Ophthalmology*. 1988;95(10):1385−1388.
8. Thompson JT. Kinetics of intraocular gases. Disappearance of air, sulfur hexafluoride, and perfluoropropane after pars plana vitrectomy. *Arch Ophthalmol*. 1989;107(5):687−691. https://doi.org/10.1001/archopht.1989.01070010705031.
9. Schwartz SG, Flynn HW. Primary retinal detachment: scleral buckle or pars plana vitrectomy? *Curr Opin Ophthalmol*. 2006;17(3):245−250.
10. Vaziri K, Schwartz SG, Kishor KS, Flynn Jr HW. Tamponade in the surgical management of retinal detachment. *Clin Ophthalmol*. 2016;10:471−476.
11. Silvanus M-T, Moldzio P, Bornfeld N, Peters J. Visual loss following intraocular gas injection. *Dtsch Arztebl Int*. 2008;105(6):108−112.
12. Butler WP, Steinkraus LW, Burlingame EE, et al. Clinical impact of cabin altitude restriction following aeromedical evacuation. *Mil Med*. 2018;183(Suppl 1):193−202.
13. Fang IM, Huang J-S. Central retinal artery occlusion caused by expansion of intraocular gas at high altitude. *Am J Ophthalmol*. 2002;134(4):603−605.
14. Foulsham W, Chen XN, Vavvas DG. Altitude-associated intraocular pressure changes in a gas-filled eye. *Retin Cases Brief Rep*. 2021;15(5):564−567.
15. Miller JB, Papakostas TD, Vavvas DG. Complications of emulsified silicone oil after retinal detachment repair. *Semin Ophthalmol*. 2014;29(5−6):312−318.
16. Muni RH, Felfeli T, Sadda SR, et al. Postoperative photoreceptor integrity following pneumatic retinopexy vs pars plana vitrectomy for retinal detachment repair: a post hoc optical coherence tomography analysis from the Pneumatic Retinopexy Versus Vitrectomy for the Management of Primary Rhegmatogenous Retinal Detachment Outcomes Randomized Trial. *JAMA Ophthalmol*. 2021;139(6):620−627.
17. Martinez-Castillo V, Zapata MA, Boixadera A, et al. Pars plana vitrectomy, laser retinopexy, and aqueous tamponade for pseudophakic rhegmatogenous retinal detachment. *Ophthalmology*. 2007;114(2):297−302.
18. Heriot W. Thermofusion of the retina with the RPE to seal tears during retinal detachment repair. *Graefes Arch Clin Exp Ophthalmol*. 2016;254(4):691−696.
19. Stappler T, Williams R, Gibran S, et al. A guide to the removal of heavy silicone oil. *Br J Ophthalmol*. 2008;92(6):844−847.
20. Bertie JE, Lan Z. Infrared intensities of liquids XX: the intensity of the oh stretching band of liquid water revisited, and the best current values of the optical constants of H20(1) at 25°C between 15,000 and 1 cm-1. *Appl Spectrosc*. 1996;50(8):1047−1057.
21. Zarei R, Azimi R, Moghimi S, et al. Inhibition of intraocular fibrin formation after infusion of low-molecular-weight heparin during combined phacoemulsification-trabeculectomy surgery. *J Cataract Refract Surg*. 2006;32(11):1921−1925.
22. Sakamoto T, Ishibashi T. Visualizing vitreous in vitrectomy by triamcinolone. *Graefes Arch Clin Exp Ophthalmol*. 2009;247(9):1153−1163.
23. Los LI, van Luyn MJ, Nieuwenhuis P. Organization of the rabbit vitreous body: lamellae, Cloquet's channel and a novel structure, the 'alae canalis Cloqueti.' Exp Eye Res. 1999;69(3):343−350.
24. Al-Nawaiseh S, Thieltges F, Liu Z, et al. A step by step protocol for subretinal surgery in rabbits. *J Vis Exp*. 2016;(115):53927.
25. Chen S-N, Hwang J-F, Tseng L-F, Lin C-J. Subthreshold diode micropulse photocoagulation for the treatment of chronic central serous chorioretinopathy with juxtafoveal leakage. *Ophthalmology*. 2008;115(12):2229−2234.
26. Leggat PA, Smith DR, Kedjarune U. Surgical applications of cyanoacrylate adhesives: a review of toxicity. *Aust N Z J Surg*. 2007;77(4):209−213.
27. Tseng Y-C, Tabata Y, Hyon S-H, Ikada Y. In vitro toxicity test of 2-cyanoacrylate polymers by cell culture method. *J Biomed Mater Res*. 1990;24(10):1355−1367.
28. Sirimaharaj M, Balachandran C, Chan WC, et al. Vitrectomy with short term postoperative tamponade using perfluorocarbon liquid for giant retinal tears. *Br J Ophthalmol*. 2005;89(9):1176−1179.
29. Martínez-Castillo V, Zapata M, Boixadera A, et al. Pars plana vitrectomy, laser retinopexy, and aqueous tamponade for pseudophakic rhegmatogenous retinal detachment. *Ophthalmology*. 2007;114(2):297−302.
30. Marmor MF. Control of subretinal fluid: Experimental and clinical studies. *Eye*. 1990;4(2):340−344.
31. Shiragami C, Shiraga F, Yamaji H, et al. Unintentional displacement of the retina after standard vitrectomy for rhegmatogenous retinal detachment. *Ophthalmology*. 2010;117(1):86−92.e1.
32. Brosh K, Francisconi CLM, Qian J, et al. Retinal displacement following pneumatic retinopexy vs pars plana vitrectomy for rhegmatogenous retinal detachment. *JAMA Ophthalmol*. 2020;138(6):652−659.
33. Francisconi CLM, Marafon SB, Figueiredo NA, et al. Retinal Displacement after Pneumatic Retinopexy versus Vitrectomy for Rhegmatogenous Retinal Detachment (ALIGN). *Ophthalmology*. 2022;129(4):458−461.
34. Hillier RJ, Felfeli T, Berger AR, et al. The Pneumatic Retinopexy versus Vitrectomy for the Management of Primary Rhegmatogenous Retinal Detachment Outcomes Randomized Trial (PIVOT). *Ophthalmology*. 2019;126(4):531−539.
35. Lee WW, Bansal A, Sadda SR, et al. Outer retinal folds after pars plana vitrectomy vs. pneumatic retinopexy for retinal detachment repair: post hoc analysis from PIVOT. *Ophthalmol Retina*. 2022;6(3):234−242.
36. Bansal A, Lee WW, Felfeli T, Muni RH. Real-time in vivo assessment of retinal reattachment in humans using swept-source optical coherence tomography. *Am J Ophthalmol*. 2021;227:265−274.

37. Farahvash A, Marafon SB, Juncal VR, et al. Understanding the mechanism of retinal displacement following rhegmatogenous retinal detachment repair: a computer simulation model. *Acta Ophthalmol*. 2021; 2021 Oct 25. https://doi.org/10.1111/aos.15050. Online ahead of print.
38. Rinkoff J, Machemer R, Hida T, Chandler D. Temperature-dependent light damage to the retina. *Am J Ophthalmol*. 1986;102(4):452–462.
39. Acharya S, Rayborn ME, Hollyfield JG. Characterization of SPACR, a sialoprotein associated with cones and rods present in the interphotoreceptor matrix of the human retina: immunological and lectin binding analysis. *Glycobiology*. 1998;8(10):997–1006.
40. Hollyfield JG. Hyaluronan and the functional organization of the interphotoreceptor matrix. *Invest Ophthalmol Vis Sci*. 1999;40(12):2767–2769.
41. Coles JM, Chang DP, Zauscher S. Molecular mechanisms of aqueous boundary lubrication by mucinous glycoproteins. *Curr Opin Colloid Interface Sci*. 2010;15(6):406–416.
42. Wang ZY, Zhao PQ. Perfluorocarbon-air exchange in head side-turned position: a simple technique to avoid retinal slippage. *Retina*. 2010;30(1):177–179.